SCIENTIFIC REPORTS

OPEN

SUBJECT AREAS:
MATERIALS FOR ENERGY AND CATALYSIS
ELECTROCHEMISTRY

Received
14 September 2014

Accepted
4 December 2014

Published
7 January 2015

Correspondence and requests for materials should be addressed to L.J. (lijian@hust.edu.cn)

Electrochemical performance and carbon deposition resistance of M-$BaZr_{0.1}Ce_{0.7}Y_{0.1}Yb_{0.1}O_{3-\delta}$ (M=Pd, Cu, Ni or NiCu) anodes for solid oxide fuel cells

Meng Li, Bin Hua, Jian Pu, Bo Chi & Li Jian

Center for Fuel Cell Innovation, State Key Laboratory for Coal Combustion, School of Materials Science and Engineering, Huazhong University of Science and Technology, Wuhan, Hubei 430074, China.

Pd-, Cu-, Ni- and NiCu-$BaZr_{0.1}Ce_{0.7}Y_{0.1}Yb_{0.1}O_{3-\delta}$ anodes, designated as M-BZCYYb, were prepared by impregnating M-containing solution into BZCYYb scaffold, and investigated in the aspects of electrocatalytic activity for the reactions of H_2 and CH_4 oxidation and the resistance to carbon deposition. Impregnation of Pd, Ni or NiCu significantly reduced both the ohmic (R_Ω) and polarization (R_P) losses of BZCYYb anode exposed to H_2 or CH_4, while Cu impregnation decreased only R_Ω in H_2 and the both in CH_4. Pd-, Ni- and NiCu-BZCYYb anodes were resistant to carbon deposition in wet (3 mol. % H_2O) CH_4 at 750°C. Deposited carbon fibers were observed in Pd- and Ni-BZCYYb anodes exposed to dry CH_4 at 750°C for 12 h, and not observed in NiCu-BZCYYb exposed to dry CH_4 at 750°C for 24 h. The performance of a full cell with NiCu-BZCYYb anode, YSZ electrolyte and $La_{0.6}Sr_{0.4}Co_{0.2}Fe_{0.8}O_{3-\delta}$-Gd doped CeO_2 (LSCF-GDC) cathode was stable at 750°C in wet CH_4 for 130 h, indicating that NiCu-BZCYYb is a promising anode for direct CH_4 solid oxide fuel cells (SOFCs).

Solid oxide fuel cells (SOFCs) are considered as one of the most promising electricity generation technologies due to their ability to directly and efficiently convert chemical energy in fuels to electricity. A major advantage of SOFCs over those low temperature fuel cells such as proton exchange membrane fuel cells is the fuel flexibility because their high operation temperature facilitates the cleavage of chemical bonds to release chemical energy[1,2]. Various fuels, such as hydrogen, methane, propane, carbon monoxide and even solid carbon, can be used as potential fuels for SOFCs. Ni-YSZ cermet is the-state-of-art anode material for SOFCs, since it possesses high electrical conductivity and electrocatalytic activity for H_2 oxidation reaction[3,4]; but it is not suitable for directly utilizing hydrocarbon fuels as Ni promotes carbon deposition[5,6]. As a matter of fact, the deactivation of Ni-based anodes due to coking has been one of the main stumbling blocks for the development of SOFCs[7], and stimulated the search of anode materials that are electrochemically active for fuel oxidation and resistant towards carbon deposition.

The nature of a catalyst has significant influence on carbon formation. Ni is known to be an excellent catalyst for cracking of hydrocarbons, so that carbon species are more liable to deposit on the surfaces of Ni[8]. In order to use CH_4 with Ni-YSZ anode, extensive efforts have been made to alleviate carbon deposition, such as introducing oxides[9–12], element alloying of Ni[13–15] or adding an extra catalyst layer[16–18]. These methods enhance the resistance to carbon deposition but reduce the activity and complicate the fabrication process of the anode. For fundamentally resolving the issue associated to Ni based anodes, it is necessary to develop alternative anode materials. Gorte et al.[19,20] proposed a Ni-free anode based on Cu or Cu alloys and CeO_2 impregnated into porous YSZ scaffold. In this structure, Cu is electronically conductive and inert to carbon formation and CeO_2 is considered as the electrocatalyst for fuel oxidation. Another approach is to employ all-ceramic anodes; and highly active perovskite-type oxides, such as doped $LaCrO_3$[21,22] and doped $SrTiO_3$[23–25], have been extensively investigated. Unfortunately, these ceramic oxides have a much lower conductivity than Ni based cermets[21,23,26], and the cells

with such anodes need to be operated at higher temperatures to achieve comparable electrochemical performance.

Recently, a new perovskite-type oxide $BaZr_{0.1}Ce_{0.7}Y_{0.1}Yb_{0.1}O_{3-\delta}$ (BZCYYb) has exhibited satisfying carbon deposition resistance and electrochemical performance at lower temperatures than other oxide anodes in both hydrogen and methane[27]. In order to use BZCYYb anode in practical cells, the anode ohmic resistance needs to be further decreased. Solution impregnation of conductive nano-particles into BZCYYb porous scaffold is expected to be effective on significantly enhancing the electronic conductivity of the anode as wet impregnation technique is a well-known technique for preparation of nano-structured electrodes in SOFCs[28–30]. In the present study, composite anodes were prepared by impregnating Pd, Cu, Ni and NiCu alloy nano-particles, respectively, into BZCYYb scaffold and investigated in the aspects of ohmic resistance, electrochemical activity and carbon deposition resistance.

Results

Microstructures of impregnated composite anodes. All the composite anodes used in this study were prepared by introducing 10 wt. % metallic oxide particles into porous BZCYYb scaffold through solution impregnation, denoted by M-BZCYYb (M = Pd, Cu, Ni or NiCu). Their cross-sectional microstructures prior to reduction are shown in Fig. 1. The infiltrated Cu oxide nanoparticles were in the range from 40 to 70 nm but poorly distributed in aggregates (Fig. 1a), which may suggest that the interfacial energy between CuO and the scaffold is relatively high, resulting in particle agglomeration during the fabrication processes. Differently, impregnated Pd (Fig. 1b), Ni (Fig. 1c) and NiCu (Fig. 1d) oxides, in the range from 30 to 50 nm, were uniformly distributed on the surface of BZCYYb scaffold, which did not obviously decrease the porosity of BZCYYb scaffold and ensured the access of fuel gas to the inner surface of the anodes. From the viewpoint of microstructure, Pd-BZCYYb, Ni-BZCYYb and NiCu-BZCYYb are more preferred than Cu-BZCYYb.

H_2 and CH_4 oxidation on M-BZCYYb anodes. Fig. 2 shows the open circuit electrochemical impedance spectra (EIS) of H_2 oxidation reaction on M-BZCYYb anodes at temperatures from 650 to 750°C. For comparison, the EIS of pure BZCYYb anode were also illustrated. It is noted that the ohmic loss (R_Ω), determined by the high-frequency intercept at the real axis, decreased dramatically due to the impregnation of metallic oxides that were reduced to metals during EIS test. For example, the value of R_Ω was 5.54, 3.42 and 2.51 Ω cm² for the cell with pure BZCYYb anode at 650, 700 and 750°C, respectively; and it was 4.27, 2.67 and 2.06 Ω cm² for that with Ni-BZCYYb anode at the same temperatures. For a 1.3 mm thick BZCYYb electrolyte, the calculated ohmic resistance at 700°C is 2.6 Ω cm², which is lower than the measured R_Ω that includes the contributions from both the electrolyte and electrode[31]. With Ni impregnation the difference decreased from 0.82 to 0.07 Ω cm², suggesting that the electrode contribution to ohmic resistance was significantly reduced. Table 1 summaries the polarization resistance (R_P) of all the anodes, determined by the difference between the high- and low-frequency intercept at the real axis, at various temperatures. Except for Cu-BZCYYb, the value of R_P for M-BZCYYb anodes decreased in comparison with that for BZCYYb anode, indicating that impregnating metal oxide into BZCYYb scaffold improved the electrocatalytic activity of the anodes, and Ni and NiCu alloy were much more effective than Pd. This result is consistent with what reported in prior publications, that is, Ni is more catalytically active for H_2 dissociation than Pd[32] and the activity of NiCu alloy is equivalent to that of Ni[14]. Cu is inert for the reaction of H_2 oxidation, and therefore did not positively affect the electrochemical performance of the anode.

Fig. 3 shows the open circuit EIS of the prepared anodes in wet CH_4 atmosphere at temperatures ranging from 650 to 750°C, and the corresponding values of R_P for each anode are also listed in Table 1. Compared with pure BZCYYb anode, both ohmic and polarization resistance of all the M-BZCYYb anodes decreased significantly. Even for Cu-BZCYYb anode, the value of R_p declined to the range between 3.54 and 0.87 Ω cm² from that between 5.24 and 0.93 Ω cm² for pure BZCYYb anode at temperatures between 650 and 750°C.

Carbon deposition in M-BZCYYb anodes. Pd-, Ni- and NiCu-BZCYYb anodes were further evaluated at open circuit in both wet

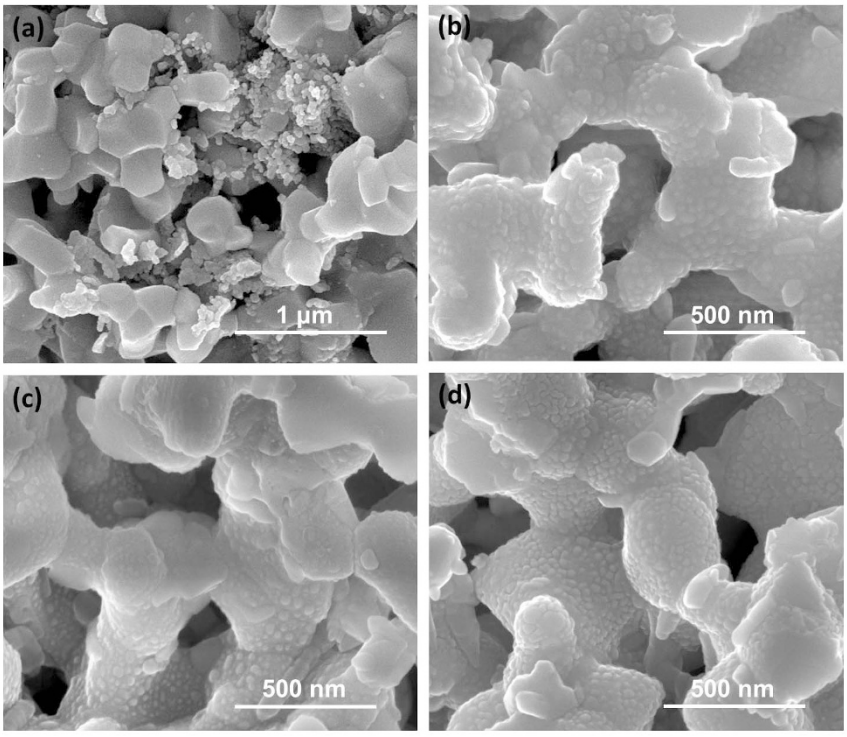

Figure 1 | Cross-sectional microstructure of M-BZCYYb anodes: (a) Cu-BZCYYb; (b) Pd-BZCYYb; (c) Ni-BZCYYb and (d) NiCu-BZCYYb.

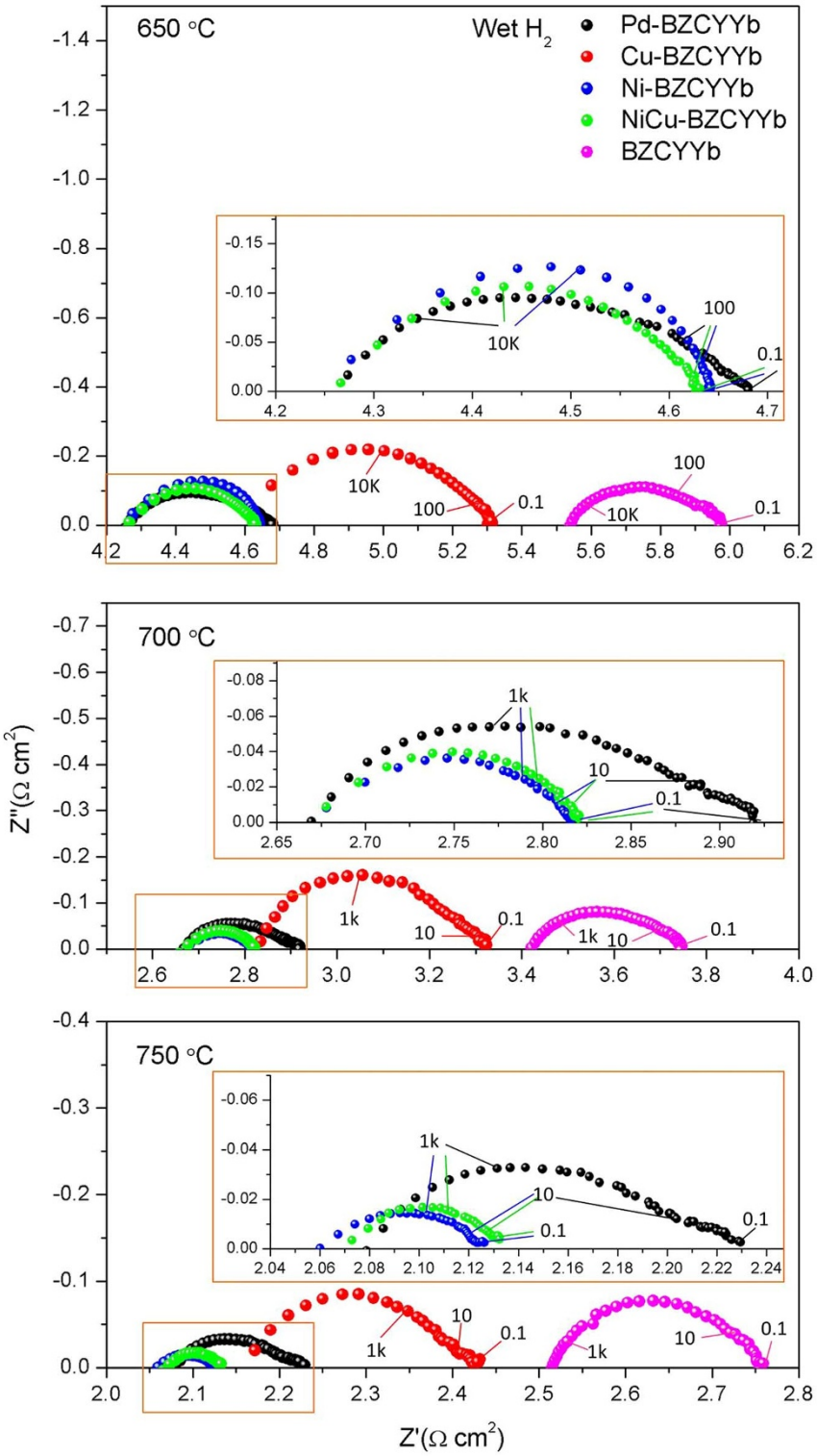

Figure 2 | **Open circuit EIS of BZCYYb and M-BZCYYb anodes exposed to wet H_2 at temperatures from 650 to 750°C.**

Table 1 | Polarization resistance for oxidation reactions of wet H_2 and CH_4 on BZCYYb and M-BZCYYb anodes

		R_p (Ω cm²)				
	Temperature (°C)	BZCYYb	Pd-BZCYYb	Cu-BZCYYb	Ni-BZCYYb	NiCu-BZCYYb
H_2	650	0.44	0.42	0.73	0.390	0.370
	700	0.33	0.25	0.49	0.149	0.152
	750	0.25	0.15	0.27	0.066	0.064
CH_4	650	5.24	2.50	3.54	2.12	2.34
	700	2.32	1.18	1.79	0.96	1.03
	750	0.93	0.62	0.87	0.57	0.60

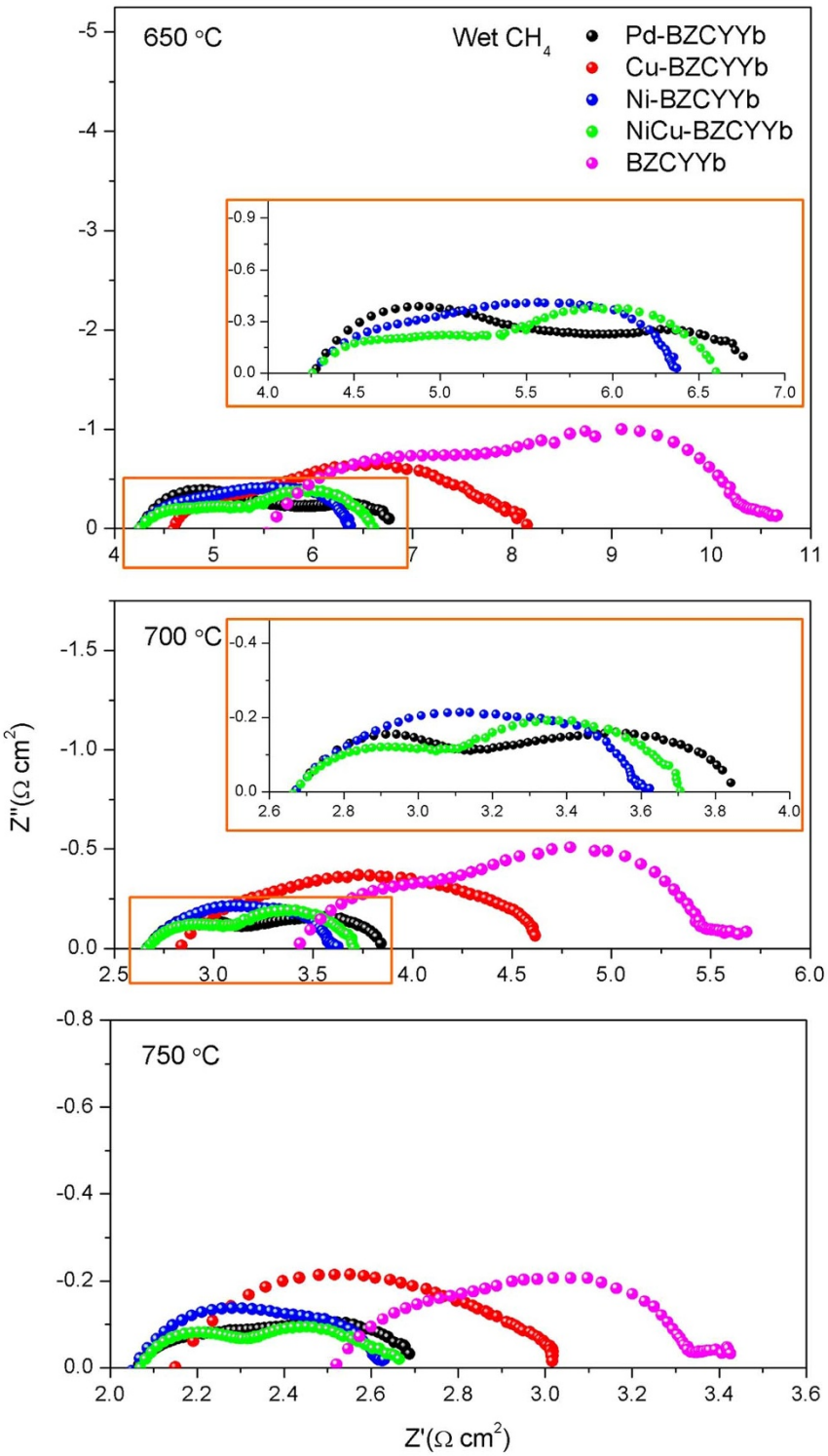

Figure 3 | Open circuit EIS of BZCYYb and M-BZCYYb anodes exposed to wet CH_4 at temperatures from 650 to 750°C.

and dry CH_4, respectively, to understand their resistance to carbon deposition. The wet CH_4 contained 3 mol. % of H_2O. Raman spectroscopy was employed to detect the presence of carbon in the tested anodes. The results shown in Fig. 4 indicates that there was no carbon formation in Pd-, Ni- and NiCu-BZCYYb anodes after exposed to wet CH_4 for up to 24 h at 750°C (Fig. 4a), and deposited carbon was found in Pd- and Ni-BZCYYb anodes after 12 h exposure in dry CH_4 featured by the peaks at about 1350 cm^{-1} (D: disordered carbon) and 1580 cm^{-1} (G: graphitic carbon), rather than in NiCu-BZCYYb anode even exposed in dry CH_4 for 24 h (Fig. 4b). Fig. 5 shows the cross-sectional microstructures of above three anodes exposed to wet and dry CH_4. The microstructures of the anodes tested in wet CH_4 for 24 h was featured by metallic nanoparticles uniformly deposited on BZCYYb scaffold (Fig. 5a–c) without the presence of deposited carbon; however, deposited carbon fibers were observed in both Pd- and Ni-BZCYYb anodes (Fig. 5d and 5e), but not in NiCu-BZCYYb anode (Fig. 5f). The microstructure observation is consistent with the results of Ramann spectroscopy. In consideration of both the electrocatalytic activity and the resistance to carbon deposition, NiCu-BZCYYb is

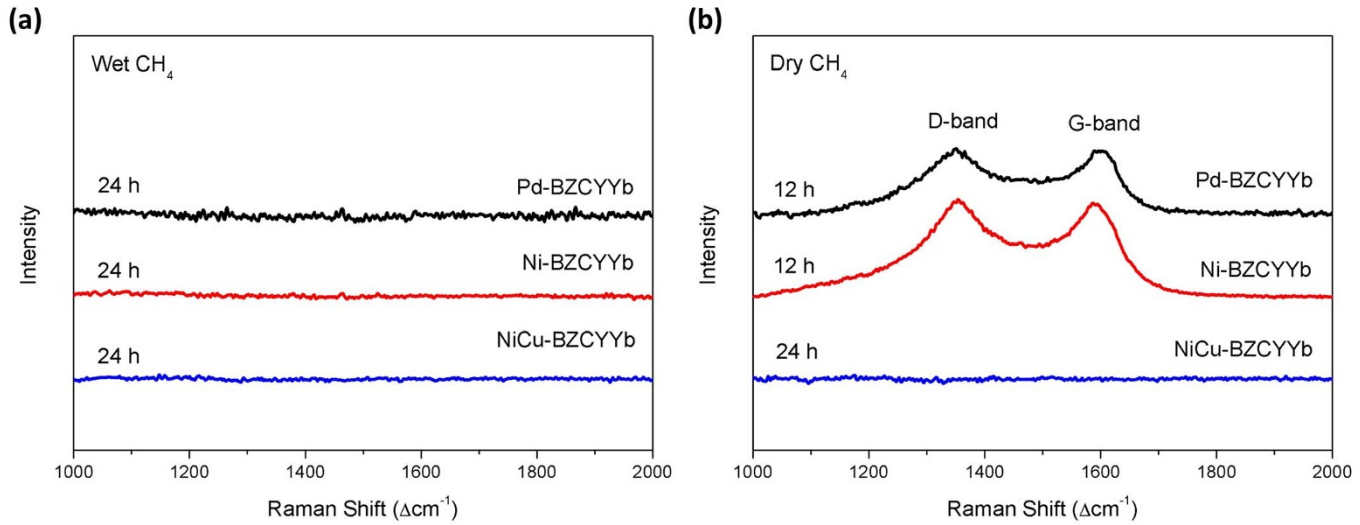

Figure 4 | **Raman spectra of M-BZCYYb anodes exposed to (a) wet CH_4 and (b) dry CH_4 at 750°C for various durations of time.**

the desired anode for SOFCs fueled by CH_4, and was subjected to a full cell test as shown below.

Cell performance. The cell consisting of NiCu-BZCYYb anode, YSZ electrolyte and $La_{0.6}Sr_{0.4}Co_{0.2}Fe_{0.8}$-Gd doped CeO_2 (LSCF-GDC) cathode was evaluated with wet CH_4 as the fuel and air as the oxidant. Fig. 6 shows its initial performance at 650, 700 and 750°C (Fig. 6a) and performance durability at 200 mA cm^{-2} and 750°C for up to 130 h (Fig. 6b). The open circuit voltage of the cells was around 1.04–1.08 V, and the peak power density was 17, 47 and 106 mW cm^{-2} at 650, 700 and 750°C, respectively. It is realized that the cell was supported on a 200 μm thick YSZ electrolyte; the majority of the losses of the cell is associated with the ohmic loss contributed by the electrolyte. If a thin YSZ electrolyte, such as 10 μm, were used in the cell, significant improvement of cell performance would have been expected. Since the purpose of the present study was to evaluate the carbon deposition resistance of the anode, performance durability of the cell was the point of concern. It is noted that the cell performance remained perfectly stable after initial increase due to the cathode activation[33,34] and the I-V and power curves slightly increased with testing time at 65 and 130 h, which again confirms that NiCu-BZCYYb is a carbon deposition resistant anode for SOFCs. Fig. 7 shows the cross-sectional microstructure of the NiCu-BZCYYb anode in the cell used for the durability test. The size of NiCu particles was in the range between 70 and 150 nm, which is slightly larger than the original without compromising the performance.

Discussion

It is known that the ohmic loss R_Ω of a cell is mainly contributed by the resistance of electrolyte, since conventional electrode materials are mixed ionic and electronic conductors as required. However, BZCYYb is not a good electronic conductor, its contribution as an anode to the ohmic resistance of the cell cannot be neglected. Solution impregnation introduces metallic oxides into BZCYYb scaffold; and the interconnected oxide particles are reduced during the test to form electronic paths on the surface of the scaffold, which

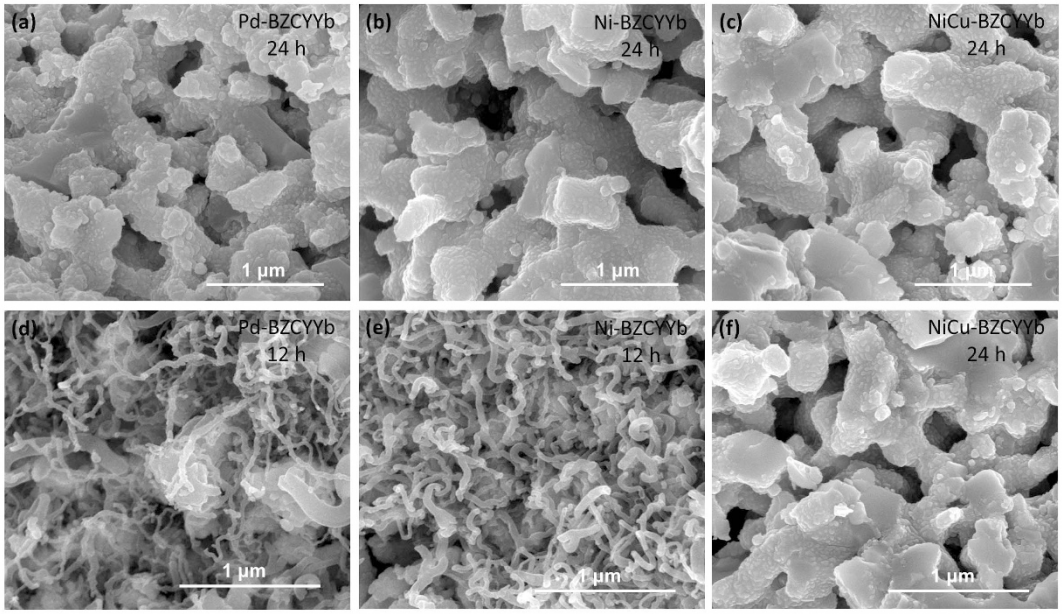

Figure 5 | **Cross-sectional microstructure of M-BZCYYb anodes exposed to wet (a, b, c) and dry (e, f, d) CH_4 at 750°C for various durations of time.**

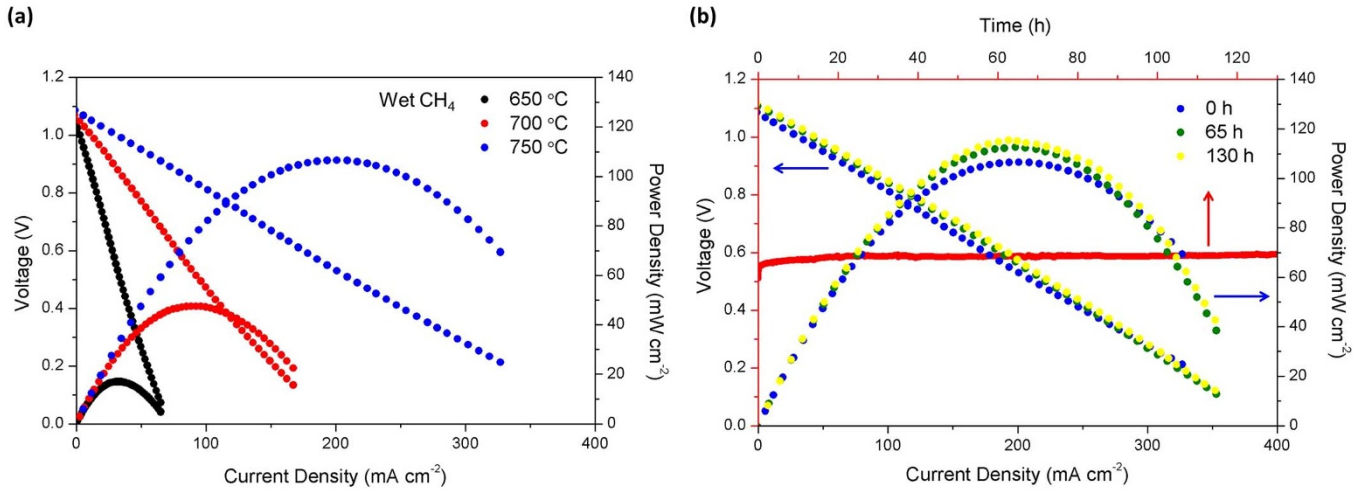

Figure 6 | Electrochemical performance of NiCu-BZCYYb anode in wet CH_4: (a) I-V/power curves at various temperatures; (b) time dependent I-V/power curves and cell voltage at 200 mA cm^{-2} at 750°C.

decreases the ohmic resistance of the anode and in turn explains the decrease in ohmic loss of the cell as shown in Fig. 2 and 3. The distribution of Pd, Ni and NiCu oxide particles is much more uniform than that of CuO, as demonstrated in Fig. 1; therefore the ohmic resistance of the Pd-, Ni- and NiCu-BZCYYb anodes is lower than that of Cu-BZCYYb anode.

Cu is ineffective on the reaction of H_2 oxidation, its function in H_2 is solely for increasing electronic conductivity of the anode. That is why the polarization loss of the anode in H_2 cannot be lowered by adding Cu into BZCYYb. Nevertheless Cu is active for the reactions of CH_4 reforming[35,36],

$$CH_4 + H_2O \rightarrow 3H_2 + CO \quad (1)$$

$$CH_4 + 2H_2O \rightarrow 4H_2 + CO_2 \quad (2)$$

Therefore, CH_4 was reformed in advance, which may facilitate the following anode reaction and decreases the polarization loss of the anode in wet CH_4, as shown in Fig. 3 and Table 1. Different from Cu, Pd, Ni and NiCu are active for both H_2 and CH_4 oxidation reactions by facilitating their adsorption and dissociation as well as electron transfer processes[16,37,38], which results in an enhanced performance of Pd-, Ni- and NiCu-BZCYYb anodes (Table 1).

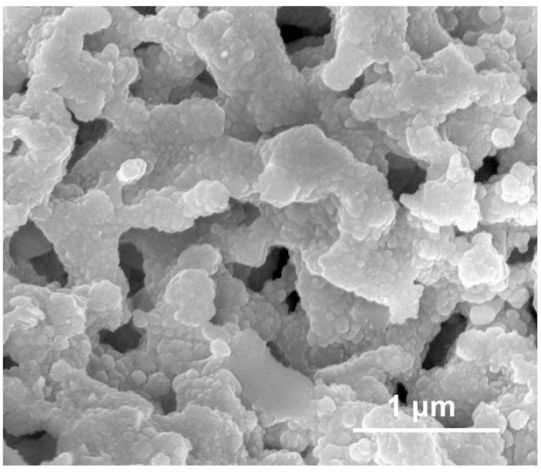

Figure 7 | Cross-sectional microstructure of the NiCu-BZCYYb anode after the durability test.

Pd and Ni are known to be excellent catalysts for CH_4 reforming accompanied with carbon deposition if the steam/carbon ratio is low[39,40]. This explains the presence of carbon fibers in Ni- and Pd-BZCYYb tested in dry CH_4 (Fig. 4b, Fig. 5d and 5e). With 3 mol. % of H_2O added in CH_4, the steam/carbon ratio is still lower than that thermodynamically required for avoiding carbon deposition. However, BZCYYb can absorb H_2O on its surface[40] to increase the local H_2O content for carbon removal; as a result carbon fibers are not observed (Fig. 4a, Fig. 5a and 5b). NiCu alloy particles are enriched on the surface with Cu[41,42], which is a poor catalyst for C-C bond formation. This prevents carbon deposition in NiCu-BZCYYb anode exposed to both wet and dry CH_4 (Fig. 4, Fig. 5c and 5f) for up to 130 h (Fig. 7b).

From above results and discussion, the following conclusions are made.

1. The electrocatalytic activity of the impregnated anodes for the reaction of H_2 oxidation is largely due to the nano-scale Pd, Ni, NiCu catalysts, which decrease both the ohmic and polarization resistance of the anodes. Cu is ineffective for the reaction of H_2 oxidation, and can only make contribution to the anode for the increase of electronic conductivity.
2. The electrochemical performance of BZCYYb anode in wet CH_4 can be improved by solution impregnation of Pd, Cu, Ni or NiCu oxide particles. Carbon deposition in Pd- and Ni-BZCYYb anodes is depressed in wet CH_4 at open circuit due to H_2O adsorption on BZCYYb; and only NiCu-BZCYYb anode is resistant to carbon deposition in both wet and dry CH_4 and can be used in full cells with wet CH_4 as the fuel.

Methods

Materials synthesis. $BaZr_{0.1}Ce_{0.7}Y_{0.1}Yb_{0.1}O_{3-\delta}$ powder used for the electrolyte was synthesized by solid state reaction of Ba, Zr, Ce, Y and Yb oxides at 1100°C, and that used for the anode was synthesized by sol-gel method with Ba, Zr, Ce, Y and Yb nitrates as the precursor. The detailed processes were described in our previous publication[27]. $Gd_{0.1}Ce_{0.9}O_{1.95}$ (GDC) and $La_{0.6}Sr_{0.4}Co_{0.2}Fe_{0.8}O_{3-\delta}$ (LSCF) powders used for the buffer and cathode were prepared by solution methods[43] with metal nitrates as the raw materials. All the chemicals used for materials synthesis were provided by Sinopharm Chemical Reagent Co., Ltd. X-ray diffraction (XRD, X'Pert Pro, PAN Analytical B.V.) was employed to confirm the phase formation.

Cell fabrication. To fabricate the half cells for electrochemical impedance measurement, BZCYYb electrolyte was used as the substrate (Φ21 × 1.3 mm), which was prepared by sintering die-pressed BZCYYb discs in air at 1450°C for 4 h. The porous BZCYYb scaffolds (0.5 cm^2) were made on one side of the substrates by screen printing of BZCYYb slurry and sintering at 1150°C in air for 1 h. Aqueous nitrate solutions (0.6 mol/L) of Pd, Cu, Ni or NiCu were subsequently impregnated into the BZCYYb scaffolds, respectively, followed by calcination in air at 750°C for 2 h for

converting the solution to metal oxides. Such prepared M-BZCYYb (M = Pd, Cu, Ni, or NiCu) composite anodes contained 10 wt. % of metal oxides. Anode microstructure was examined by using a scanning electron microscope (SEM, Nova NanoSEM 450, FEI).

The full cell was YSZ electrolyte supported with NiCu-BZCYYb as the anode and LSCF-GDC as the cathode. The YSZ electrolyte substrate (Φ 20 × 0.2 mm) was prepared by sintering tape-cast YSZ wafer in air at 1500°C for 6 h. A GDC buffer layer (<5 μm) placed on each side of the substrate by sintering screen-printed GDC paste in air at 1300°C for 10 h. The NiCu-BZCYYb anode on the GDC buffer layer was prepared as described above; and the LSCF-GDC cathode on another GDC buffer layer was prepared by sintering screen printed LSCF-GDC mixed paste (70 : 30 in weight) in air at 950°C for 2 h. The thickness of the porous NiCu-BZCYYb anode and LSCF-GDC cathode was in the range between 25 and 30 μm.

Electrochemical measurements. For the electrochemical impedance measurement, Pt (Sino-Platinum Metals Co., Ltd) was used as the counter and reference electrode prepared by baking screen-printed Pt paste on the other side of the BZCYYb substrate (symmetrically opposite to the prepared anode) in air at 750°C for 0.5 h. The gap between the round-shaped counter and ring-shaped reference electrode was 4.8 mm. Pt mesh and wire were used as the current collector and measuring lead. The anode was sealed onto the cell holder (Al_2O_3 tube) by a Ceramabond® glass sealant (Aremco Product, Inc.). Wet (3 mol.% H_2O) H_2 or CH_4 was fed to the anodes at a constant flow rate of 100 ml min^{-1}; and ambient air was supplied to the cathode at 250 ml min^{-1}. Electrochemical impedance spectra (EIS) were obtained at open circuit with voltage amplitude of 20 mV in the frequency range from 10^6 to 10^{-1} Hz by using an impedance/gain phase analyzer (Solartron 1260) and an electrochemical interface (Solartron 1287). The full cell test was conducted at 200 mA cm^{-2}. The anodes exposed to wet and dry CH_4 for various time at 750°C were subjected to SEM examination and Ramann spectroscopy (RS, LabRAM HR800, Horiba JobinYvon) for carbon detection.

1. Yi, Y., Rao, A. D., Brouwer, J. & Samuelsen, G. S. Fuel flexibility study of an integrated 25kW SOFC reformer system. *J. Power Sources* **144**, 67–76 (2005).
2. Eguchi, K., Kojo, H., Takeguchi, T., Kikuchi, R. & Sasaki, K. Fuel flexibility in power generation by solid oxide fuel cells. *Solid State Ionics* **152–153**, 411–416 (2002).
3. Lee, J. H. *et al.* Quantitative analysis of microstructure and its related electrical property of SOFC anode, Ni–YSZ cermet. *Solid State Ionics* **148**, 15–26 (2002).
4. Aruna, S. T., Muthuraman, M. & Patil, K. C. Synthesis and properties of Ni-YSZ cermet: anode material for solid oxide fuel cells. *Solid State Ionics* **111**, 45–51 (1998).
5. Irvine, J. T. S. & Sauvet, A. Improved oxidation of hydrocarbons with new electrodes in high temperature fuel cells. *Fuel Cells* **1**, 3–4 (2001).
6. Tao, S. & Irvine, J. T. S. Discovery and characterization of novel oxide anodes for solid oxide fuel cells. *Chem. Rec.* **4**, 83–95 (2004).
7. Badwal, S. P. S. Stability of solid oxide fuel cell components. *Solid State Ionics* **143**, 39–46 (2001).
8. He, H. & Hill, J. M. Carbon deposition on Ni/YSZ composites exposed to humidified methane. *Appl. Catal. A: Gen.* **317**, 284–292 (2007).
9. Huang, T.-J. & Huang, M.-C. Electrochemical promotion of bulk lattice-oxygen extraction for syngas generation over Ni-GDC anodes in direct-methane SOFCs. *Chem. Eng. J.* **135**, 216–223 (2008).
10. Sumi, H., Lee, Y.-H., Muroyama, H., Matsui, T. & Eguchi, K. Comparison between internal steam and CO_2 reforming of methane for Ni-YSZ and Ni-ScSZ SOFC anodes. *J. Electrochem. Soc.* **157**, B1118 (2010).
11. Zha, S., Moore, A., Abernathy, H. & Liu, M. GDC-based low-temperature SOFCs powered by hydrocarbon fuels. *J. Electrochem. Soc.* **151**, A1128 (2004).
12. Wang, J. B., Jang, J.-C. & Huang, T.-J. Study of Ni-samaria-doped ceria anode for direct oxidation of methane in solid oxide fuel cells. *J. Power Sources* **122**, 122–131 (2003).
13. Nikolla, E., Schwank, J. & Linic, S. Promotion of the long-term stability of reforming Ni catalysts by surface alloying. *J. Catal.* **250**, 85–93 (2007).
14. Park, E. W., Moon, H., Park, M.-S. & Hyun, S. H. Fabrication and characterization of Cu–Ni–YSZ SOFC anodes for direct use of methane via Cu-electroplating. *Int. J. Hydrogen Energy* **34**, 5537–5545 (2009).
15. Kan, H. & Lee, H. Enhanced stability of Ni–Fe/GDC solid oxide fuel cell anodes for dry methane fuel. *Catal. Commun.* **12**, 36–39 (2010).
16. Hua, B., Li, M., Chi, B. & Jian, L. Enhanced electrochemical performance and carbon deposition resistance of Ni–YSZ anode of solid oxide fuel cells by in situ formed Ni–MnO layer for CH_4 on-cell reforming. *J. Mater. Chem. A* **2**, 1150 (2014).
17. Hua, B. *et al.* Methane on-cell reforming by alloys reduced from $Ni_{0.5}Cu_{0.5}Fe_2O_4$ for direct-hydrocarbon solid oxide fuel cells. *J. Electrochem. Soc.* **161**, F569–F575 (2014).
18. Hua, B., Li, M., Pu, J., Chi, B. & Li, J. $BaZr_{0.1}Ce_{0.7}Y_{0.1}Yb_{0.1}O_{3-\delta}$ enhanced coking-free on-cell reforming for direct-methane solid oxide fuel cells. *J. Mater. Chem. A* **2**, 12576 (2014).
19. Park, S., Vohs, J. M. & Gorte, R. J. Direct oxidation of hydrocarbons in a solid-oxide fuel cell. *Nature* **404**, 265–267 (2000).
20. Gorte, R. J., Park, S., Vohs, J. M. & Wang, C. Anodes for direct oxidation of dry hydrocarbons in a solid-oxide fuel cell. *Adv. Mater.* **12**, 1465–1469 (2000).
21. Tao, S. & Irvine, J. T. A redox-stable efficient anode for solid-oxide fuel cells. *Nat. Mater.* **2**, 320–323 (2003).
22. Liu, J., Madsen, B. D., Ji, Z. & Barnett, S. A. A fuel-flexible ceramic-based anode for solid oxide fuel cells. *Electrochem. Solid-State Lett.* **5**, A122 (2002).
23. Ruiz-Morales, J. C. *et al.* Disruption of extended defects in solid oxide fuel cell anodes for methane oxidation. *Nature* **439**, 568–571 (2006).
24. Lee, S., Kim, G., Vohs, J. M. & Gorte, R. J. SOFC Anodes based on infiltration of $La_{0.3}Sr_{0.7}TiO_3$. *J. Electrochem. Soc.* **155**, B1179 (2008).
25. Neagu, D. & Irvine, J. T. S. Structure and properties of $La_{0.4}Sr_{0.4}TiO_3$ ceramics for use as anode materials in solid oxide fuel cells. *Chem. Mater.* **22**, 5042–5053 (2010).
26. Tao, S. W. & Irvine, J. T. S. Catalytic properties of the perovskite oxide $La_{0.75}Sr_{0.25}Cr_{0.5}Fe_{0.5}O_{3-\delta}$ in relation to its potential as a solid oxide fuel cell anode material. *Chem. Mater.* **16**, 4116–4121 (2004).
27. Li, M., Hua, B., Pu, J., Chi, B. & Li, J. $BaZr_{0.1}Ce_{0.7}Y_{0.1}Yb_{0.1}O_{3-\delta}$ as highly active and carbon tolerant anode for direct hydrocarbon solid oxide fuel cells. *Int. J. Hydrogen Energy* **39**, 15975–15981 (2014).
28. Jiang, S. P. A review of wet impregnation-An alternative method for the fabrication of high performance and nano-structured electrodes of solid oxide fuel cells. *Mater. Sci. Eng. A* **418**, 199–210 (2006).
29. Liu, Z. B. *et al.* Fabrication and modification of solid oxide fuel cell anodes via wet impregnation/infiltration technique. *J. Power Sources* **237**, 243–259 (2013).
30. Hua, B. *et al.* Improved microstructure and performance of Ni-based anode for intermediate temperature solid oxide fuel cells. *J. Power Sources* **247**, 170–177 (2014).
31. Yang, L. *et al.* Enhanced Sulfur and Coking Tolerance of a Mixed Ion Conductor for SOFCs: $BaZr_{0.1}Ce_{0.7}Y_{0.2-x}Yb_xO_{3-\delta}$. *Science* **326**, 126–129 (2009).
32. Nabae, Y. & Yamanaka, I. Alloying effects of Pd and Ni on the catalysis of the oxidation of dry CH_4 in solid oxide fuel cells. *Appl. Catal. A: Gen.* **369**, 119–124 (2009).
33. Baumann, F. S. *et al.* Strong performance improvement of $La_{0.6}Sr_{0.4}Co_{0.8}Fe_{0.2}O_{3-\delta}$ SOFC cathodes by electrochemical activation. *J. Electrochem. Soc.* **152**, A2074 (2005).
34. Haanappel, V. A. C., Mai, A. & Mertens, J. Electrode activation of anode-supported SOFCs with LSM- or LSCF-type cathodes. *Solid State Ionics* **177**, 2033–2037 (2006).
35. Van Hook, J. P. Methane-steam reforming. *Catal. Rev.* **21**, 1–51 (1980).
36. Lewis, W. K., Gilliland, E. R. & Reed, W. A. Reaction of methane with copper oxide in a fluidized bed. *Ind. Eng. Chem.* **41**, 1227–1237 (1949).
37. McIntosh, S., Vohs, J. M. & Gorte, R. J. Effect of precious-metal dopants on SOFC anodes for direct utilization of hydrocarbons. *Electrochem. Solid-State Lett.* **6**, A240–A243 (2003).
38. Lee, S.-I., Vohs, J. M. & Gorte, R. J. A study of SOFC anodes based on Cu-Ni and Cu-Co bimetallics in CeO_2-YSZ. *J. Electrochem. Soc.* **151**, A1319–A1323 (2004).
39. Gross, M. D., Vohs, J. M. & Gorte, R. J. Recent progress in SOFC anodes for direct utilization of hydrocarbons. *J. Mater. Chem.* **17**, 3071–3077 (2007).
40. Claridge, J. B. *et al.* A study of carbon deposition on catalysts during the partial oxidation of methane to synthesis gas. *Catal. Lett.* **22**, 299–305 (1993).
41. Alstrup, I., Petersen, U. E. & Rostrup-Nielsen, J. R. Propane hydrogenolysis on sulfur- and copper-modified nickel catalysts. *J. Catal.* **191**, 401–408 (2000).
42. Kim, H., Lu, C., Worrell, W. L., Vohs, J. M. & Gorte, R. J. Cu-Ni cermet anodes for direct oxidation of methane in solid-oxide fuel cells. *J. Electrochem. Soc.* **149**, A247 (2002).
43. Liu, Y. H. *et al.* A stability study of impregnated LSCF-GDC composite cathodes of solid oxide fuel cells. *J. Alloys Compd.* **578**, 37–43 (2013).

Acknowledgments

This project is supported by the National Natural Science Foundation of China (U1134001), the National "863" Project of China (2011AA050702) and XRD, SEM and Raman characterizations were performed with the assistance of the Analytical and Testing Center of Huazhong University of Science and Technology.

Author contributions

M.L. and B.H. conducted the experiments and prepared the manuscript; J.P. and B.C. provided suggestions and comments; J.L. discussed the results and revised the manuscript.

Additional information

Competing financial interests: The authors declare no competing financial interests.

How to cite this article: Li, M., Hua, B., Pu, J., Chi, B. & Jian, L. Electrochemical performance and carbon deposition resistance of M-$BaZr_{0.1}Ce_{0.7}Y_{0.1}Yb_{0.1}O_{3-\delta}$ (M=Pd, Cu, Ni or NiCu) anodes for solid oxide fuel cells. *Sci. Rep.* **5**, 7667; DOI:10.1038/srep07667 (2015).